Thermoelectric effect enhanced by resonant states in graphene

M. Inglot,[1] A. Dyrdał,[2] V. K. Dugaev,[1,3] and J. Barnaś[2,4]

[1]*Department of Physics, Rzeszów University of Technology, Al. Powstańców Warszawy 6, 35-959 Rzeszów, Poland*
[2]*Faculty of Physics, Adam Mickiewicz University, ul. Umultowska 85, 61-614 Poznań, Poland*
[3]*Departamento de Física and CFIF, Instituto Superior Técnico, Universidade de Lisboa, Avenida Rovisco Pais, 1049-001 Lisbon, Portugal*
[4]*Institute of Molecular Physics, Polish Academy of Sciences, ul. M. Smoluchowskiego 17, 60-179 Poznań, Poland*

Thermoelectric effects in graphene are considered theoretically with particular attention paid to the role of resonant scattering on impurities. Using the T-matrix method we calculate the impurity resonant states and the momentum relaxation time due to scattering on impurities. The Boltzmann kinetic equation is used to determine the thermoelectric coefficients. It is shown that the resonant impurity states near the Fermi level give rise to a resonant enhancement of the Seebeck coefficient and figure of merit ZT. The Wiedemann-Franz ratio deviates from that known for ordinary metals, where this ratio is constant and equal to the Lorentz number. This deviation appears for small chemical potentials and in the vicinity of the resonant states. In the limit of a constant relaxation time, this ratio has been calculated analytically for $\mu = 0$.

I. INTRODUCTION

Graphene, the first strictly two-dimensional crystal, was extensively studied in the past few years, both experimentally and theoretically. This enormous interest in graphene is a consequence of its peculiar transport properties, which follow from the very specific electronic structure of graphene [1,2]. Thermal and thermoelectric properties of graphene have become a topical issue since the first measurement of thermal conductivity in graphene by Balandin *et al.* [3]. It is known that graphene is one of the best heat conductors, with a very high thermal conductivity that is a consequence of the strong sp^2 bonding, small atomic mass, and low dimensionality [4]. A giant thermoelectric effect in graphene was also predicted theoretically [5], with the Seebeck coefficient equal to 30 mV/K.

Impurities can substantially influence graphene's energy spectrum, so the thermoelectric transport strongly depends not only on the thermal activation but also on the impurity scattering mechanism. For the case of non-resonant scattering from impurities, the thermal conductivity and thermopower have been calculated by Stauber *et al.* [6]. They have found that both these kinetic coefficients strongly depend on the density of carriers and on the effective impurity (defect) radius.

The influence of impurity scattering on the thermoelectric properties of graphene was also considered theoretically using a self-consistent t-matrix approach by Löfwander *et al.* [7]. From these considerations it follows that the measured thermopower can be used to get some information on the role of impurity scattering in graphene. The thermopower near the Dirac point was considered by Wang *et al.* [8], who obtained a relatively good agreement between experimental data and theoretical results based on the Boltzmann transport theory. These authors also showed that Mott's relation fails in the vicinity of the Dirac points in the case of high-mobility graphene, being however satisfied for a wide range of gate voltages in the regime of low carrier mobility. The thermoelectric transport properties of graphene were also considered within the model of Dirac fermions in the presence of magnetic field and disorder [9–11].

Sharapov *et al.* [12] have found that the thermopower can be remarkably enhanced by opening an energy gap in the quasiparticle spectrum of graphene. The presence of the energy gap is accompanied by the emergence of a quasiparticle scattering channel, with the relaxation time strongly dependent on energy. The thermoelectric effects were also investigated in the case of multilayer graphene. The thermopower of biased and unbiased multilayers was studied in the Slonczewski-Weiss-McClure model, where the effect of impurity scattering was treated in the self-consistent Born approximation [13]. The classical and spin Seebeck effects in single as well as in multilayer graphene on a SiC substrate were also investigated within *ab initio* methods [14,15], and by nonequilibrium molecular-dynamics simulations [16].

Transport properties of graphene nanoribbons (GNRs) can be different from those of the corresponding two-dimensional graphene plane, mainly due to edge states and energy gaps which develop in the electronic spectrum due to confinement. In addition, the transport properties of GNRs also depend on the edge shape. Thermoelectric properties of GNRs have been investigated as well, and it has been shown that the thermopower in GNRs can be remarkably larger than that in planar graphene [17]. Moreover, the corresponding figure of merit, ZT, can be enhanced by introducing randomly distributed hydrogen vacancies into completely hydrogenated GNRs [18]. Structural defects, especially in the form of antidots, were also shown to be a promising way of enhancing thermoelectric efficiency in GNRs [19–23]. In the case of graphene nanowiggles (assembled graphene nanoribbons), a special arrangement of the graphene patches can also affect the figure of merit [24].

In this paper we focus on the electronic part of thermal properties of graphene. When calculating the figure of merit we include, however, the phonon term in the heat conductivity. Such a term has been already discussed in details in several papers (see, e.g., Refs. [25–28]). Apart from this, it has been shown that the electronic term in the heat conductivity can be dominant in devices of nanometer size, and this was also confirmed experimentally in Refs. [29,30].

In our consideration we take into account impurities which lead to resonant states near the Fermi level. We show that the resonant states result in a resonant enhancement of the Seebeck coefficient. This enhancement can be observed, for instance, when the Fermi level is tuned by an external gate voltage. In our description we neglect the electron-electron interactions. The effect of such an interaction on the thermal transport in graphene has been discussed recently by Principi et $al.$ [31], where possible violation of the Wiedemann-Franz law also has been discussed.

In Sec. II we describe the model and theoretical method used to calculate the Seebeck coefficient. The relaxation time is calculated in Sec. III. Numerical results on the thermoelectric transport properties are presented and discussed in Sec. IV. The Wiedemann-Franz law is briefly discussed in Sec. V, while the final conclusions are in Sec. VI.

II. MODEL

In a clean (defect-free) graphene, the electronic states in the vicinity of the Dirac points can be described by the following low-energy Hamiltonian [32]:

$$\hat{H}_0 = -i\hbar v \left(\sigma_x \nabla_x + \sigma_y \nabla_y \right), \tag{1}$$

where v is the electron velocity in graphene, and σ_x, σ_y are the Pauli matrices defined in the two-sublattice space of graphene. This Hamiltonian describes two electron energy bands with linear dispersion, $\varepsilon^{(1,2)}(\mathbf{k}) = \pm \hbar v k$. The electron velocity in each of the bands is $\mathbf{v}^{(1,2)}(\mathbf{k}) = \pm v \mathbf{k}/k$.

Assume that temperature gradient ∇T and external electric field E are oriented along the axis x. Both ∇T and E drive the system out of equilibrium. To calculate the distribution function $f^{(n)}(\mathbf{r},\mathbf{k})$ of electrons in the nth energy band in the nonequilibrium situation, we apply the Boltzmann kinetic equation. For a small deviation $\delta f^{(n)}$ of the distribution function from the equilibrium distribution f_0, the Boltzmann equation for $\delta f^{(n)}$ can be written in the relaxation time approximation as

$$v_x^{(n)} \left(-\frac{\partial f_0}{\partial \varepsilon} \right) \left(\nabla \mu + \frac{\varepsilon - \mu}{T} \nabla T - eE \right) = -\frac{\delta f^{(n)}}{\tau^{(n)}}, \tag{2}$$

where $f^{(n)}(\mathbf{r},\mathbf{k}) = f_0 + \delta f^{(n)}$, $\tau^{(n)}$ is the relaxation time in the nth band, while μ is the chemical potential, which may be spatially inhomogeneous along the axis x and thus $\nabla \mu = \partial \mu / \partial x$ is a driving force as well.

Using the solution of Eq. (2), one can find the electric current density j and the energy flux density J_E along the axis x, induced by the driving forces E, ∇T, and $\nabla \mu$ [33],

$$j = e \sum_{n\mathbf{k}} v_x^{(n)} \delta f^{(n)} = e^2 K_{11} E$$
$$- eK_{11} T \nabla \frac{\mu}{T} - eK_{21} \frac{\nabla T}{T}, \tag{3}$$

$$J_E = \sum_{n\mathbf{k}} v_x^{(n)} \varepsilon^{(n)} \delta f^{(n)} = eK_{21} - K_{21} T \nabla \frac{\mu}{T} - K_{31} \frac{\nabla T}{T}, \tag{4}$$

where K_{rs} are the kinetic coefficients for graphene,

$$K_{rs} = -\frac{1}{4\pi \hbar^2} \int_{-\infty}^{\infty} |\varepsilon| \, \varepsilon^{r-1} \tau^s(\varepsilon) \frac{\partial f_0}{\partial \varepsilon} \, d\varepsilon. \tag{5}$$

The integral in Eq. (5) runs over both energy bands, so $\tau(\varepsilon)$ is equal to $\tau^{(1)}(\varepsilon)$ for $\varepsilon > 0$, and $\tau(\varepsilon) = \tau^{(2)}(\varepsilon)$ for $\varepsilon < 0$. Note, that the heat current density J_Q is defined as $J_Q = J_E - \mu j$, so that $J_Q = J_E$ when $j = 0$.

The thermoelectric Seebeck coefficient α and the heat conductivity κ are defined from the relations $E^\alpha = \alpha \nabla T$ and $J_Q = -\kappa \nabla T$ when $j = 0$. Here, E^α is the electric field due to the temperature gradient. In general, there is also a field related to the chemical potential inhomogeneity, $E^\mu = \nabla \mu / e$, so that the total internal electric field for $j = 0$ is $E = E^\mu + E^\alpha$. This leads to the standard expressions for the electrical conductivity σ, thermoelectric Seebeck coefficient α, and heat conductance κ [33],

$$\sigma = e^2 K_{11}, \tag{6}$$

$$\alpha = \frac{K_{21} - \mu K_{11}}{e \, T \, K_{11}}, \tag{7}$$

$$\kappa_e = \frac{K_{31} K_{11} - K_{21}^2}{T K_{11}}, \tag{8}$$

which are valid for graphene when the kinetic coefficients K_{rs} are calculated from Eq. (5).

To calculate the thermoelectric parameters, Eqs. (6)–(8), it is necessary to know the energy dependence of the relaxation time due to electron scattering from impurities and defects. This problem is considered in the next section.

III. MOMENTUM RELAXATION TIME

The total Hamiltonian of graphene with impurities is $\hat{H} = \hat{H}_0 + \sum_i \hat{V}(\mathbf{r} - \mathbf{R}_i)$, where $\hat{V}(\mathbf{r} - \mathbf{R}_i)$ is a scattering potential of a single impurity located at $\mathbf{R}_i$, and the summation runs over all randomly distributed impurities. We consider the situation when the short-range-potential impurities are distributed randomly with equal probabilities in the sublattices A and B of the graphene. Correspondingly, the single-impurity perturbation is either $\hat{V}^A(\mathbf{r})$ or $\hat{V}^B(\mathbf{r})$, where

$$\hat{V}^{A(B)}(\mathbf{r}) = \hat{V}_0^{A(B)} \delta(\mathbf{r} - \mathbf{R}_{A(B)}) \tag{9}$$

and $\hat{V}_0^{A(B)} = V_0(\sigma_0 \pm \sigma_z)/2$. Here, V_0 is the impurity potential strength, σ_0 is the unit matrix in the sublattice space and $\mathbf{R}_A$ ($\mathbf{R}_B$) is a position vector of the impurity located in the sublattice A (B).

The influence of a single impurity on the energy spectrum and on the momentum relaxation time can be described in terms of the T-matrix method [34]. The T-matrix equation in the general case takes the form

$$\hat{T}_{\mathbf{k}\mathbf{k}'}(\varepsilon) = \hat{V}_{\mathbf{k}\mathbf{k}'} + \sum_{\mathbf{k}''} \hat{V}_{\mathbf{k}\mathbf{k}''} \hat{G}_{\mathbf{k}''}(\varepsilon) \hat{T}_{\mathbf{k}''\mathbf{k}'}. \tag{10}$$

where

$$\hat{G}_{\mathbf{k}}(\varepsilon) = \frac{\varepsilon + \boldsymbol{\sigma} \cdot \mathbf{k}}{(\varepsilon + i\delta)^2 - (\hbar v k)^2} \tag{11}$$

is the retarded Green's function of electrons in graphene described by the Hamiltonian $\hat{H}_0$.

In the case of short-range impurities, one can find from Eq. (10) the T matrix in the following form:

$$\hat{T}^{A,B}(\varepsilon) = \frac{\hat{V}_0^{A,B}}{1 - V_0 F(\varepsilon)}, \qquad (12)$$

where $F(\varepsilon)$ is defined as

$$F(\varepsilon) = \sum_{\mathbf{k}} \frac{\varepsilon}{(\varepsilon + i\delta)^2 - (\hbar v k)^2}. \qquad (13)$$

Using Eq. (12), and averaging over the impurity positions (assuming the same probability to find an impurity in the sublattices A and B), we find the self-energy due to scattering on randomly distributed impurities in the form

$$\hat{\Sigma}(\varepsilon) = \frac{N_i V_0 \sigma_0}{2\left[1 - V_0 F(\varepsilon)\right]}, \qquad (14)$$

where N_i is the impurity concentration.

To find the relaxation time in the nth energy band ($n = 1,2$), we have to diagonalize the operator $\hat{H}_{\text{eff}} \equiv \hat{H}_0 + \hat{\Sigma}(\varepsilon)$. Since the self-energy (14) is proportional to the unit matrix σ_0, the operator $\hat{H}_{\text{eff}}$ is diagonalized by the same transformation as $\hat{H}_0$. In other words, the electron relaxation time can be found directly from Eq. (14) as

$$\frac{\hbar}{\tau(\varepsilon)} = \text{Im} \frac{N_i V_0}{1 - V_0 F(\varepsilon)}. \qquad (15)$$

The above formula can be rewritten as

$$\frac{\hbar}{\tau(\varepsilon)} = \frac{N_i V_0^2 \left|\text{Im} F(\varepsilon)\right|}{[1 - V_0 \,\text{Re}\, F(\varepsilon)]^2 + V_0^2 [\text{Im}\, F(\varepsilon)]^2}, \qquad (16)$$

where the real and imaginary parts of $F(\varepsilon)$ can be calculated from Eq. (13):

$$\text{Re}\, F(\varepsilon) \simeq -\frac{\varepsilon}{2\pi(\hbar v)^2} \ln \frac{\hbar v k_m}{|\varepsilon|}, \qquad (17)$$

$$\text{Im}\, F(\varepsilon) \simeq -\frac{\varepsilon}{4(\hbar v)^2}. \qquad (18)$$

Here, k_m is a maximum value of the wave vector (cutoff) in graphene, $k_m = (|\mathbf{K}| + |\mathbf{M}|)/2$, with $\mathbf{K}$ and $\mathbf{M}$ denoting the wave vectors corresponding to the points K and M of the graphene Brillouin zone.

The energy of resonant states localized at an impurity can be found from the equation $\text{Re}\,\{1 - V_0 F(\varepsilon)\} = 0$. Figure 1(a) presents the energy of resonant states as a function of the normalized impurity potential V_0/V_c, where $V_c = t a_0^2$, and $t = 3$ eV is the nearest-neighbor hopping integral while $a_0 = 1.42$ Å is the carbon-carbon distance in graphene. Note that the impurity potential strength $V_0 \to \pm\infty$ corresponds to the model of a vacancy in graphene. The resonance levels have negative energy for positive V_0, i.e., they are localized below the Fermi level, while for $V_0 < 0$ the resonance levels have positive energy [35]. The resonant state of a particular energy strongly affects the energy dependence of the momentum relaxation time $\tau(\varepsilon)$, as shown in Fig. 1(b). In this figure the relaxation time is shown for three resonant states corresponding to the points in Fig. 1(a). It is clearly visible that the relaxation time is strongly suppressed at the corresponding
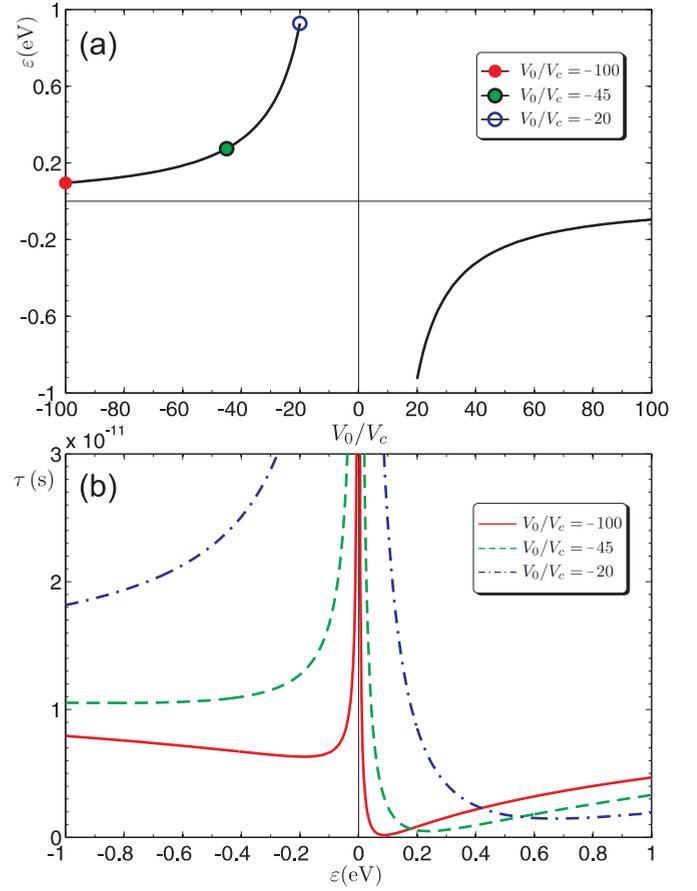

FIG. 1. (Color online) (a) Energy of the resonant states as a function of the impurity potential V_0/V_c. (b) Momentum relaxation time τ as a function of electron energy ε, calculated for the impurity concentration $N_i = 2 \times 10^{14}$ m^{-2}, and for the resonant states (and V_0/V_c) corresponding to the points marked in (a).

resonance. Note that the relaxation time becomes divergent at the the Fermi level (Dirac points). Accordingly, transport properties are also strongly dependent on the presence of resonance states.

IV. NUMERICAL RESULTS: THERMOPOWER AND FIGURE OF MERIT *ZT*

Using Eqs. (3)–(5) we calculate first the electric current for $E = 0$ and homogeneous chemical potential, $\nabla\mu = 0$. The current is then solely induced by the temperature gradient, $j = \sigma\alpha\nabla T$. In the following calculations we assume the parameters $\hbar v = 1.05 \times 10^{-28}$ J m, $k_m = 1.59 \times 10^{10}$ m^{-1}, $N_i = 2 \times 10^{14}$ m^{-2}, and $\nabla T = 8000$ K/m. Figure 2(a) presents the thermoelectric current as a function of the chemical potential μ, calculated for $T = 300$ K and for the resonance levels corresponding to the indicated values of the impurity potential V_0/V_c. Note that $\mu = 0$ corresponds to Fermi level E_F of pristine graphene ($E_F = 0$). The electrochemical potential can be tuned experimentally by an external gate voltage. As follows from Fig. 2(a), the magnitude of current as well as its variation with the chemical potential μ strongly depend on the impurity potential V_0, i.e., on the position of the resonance level.
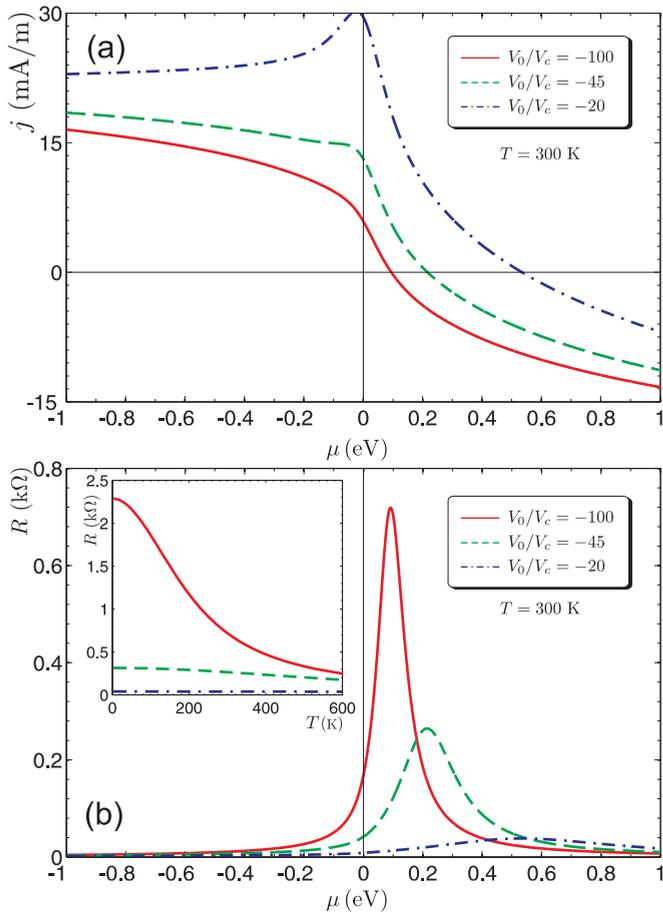
FIG. 2. (Color online) (a) Current induced by the temperature gradient ∇T as a function of the chemical potential μ, calculated for $T = 300$ K and for the indicated values of the impurity potential V_0/V_c (i.e., for the corresponding resonance levels). (b) Resistivity of graphene vs μ for $T = 300$ K and indicated values of V_0/V_c. The inset in (b) shows the corresponding resistivity vs temperature for chemical potentials corresponding to the resistance maxima in (b). The other parameters are assumed as described in the main text.

Dependence of the thermoelectric current on the chemical potential μ is closely related to the presence of resonance states. This can be also seen from the resistivity behavior, which has a pronounced maximum when the chemical potential is close to the energy of the resonance impurity state; see Fig. 2(b). From the preceding section we know that location of the resonance states is determined by the magnitude of the impurity potential V_0 [35]. To understand behavior of the thermocurrent one should note that particles and holes flow from the higher temperature to the lower one (from right to left for the assumed temperature gradient). Figure 2 shows that the thermocurrent vanishes at the chemical potential, where the resistance achieves a maximum value, i.e., when the chemical potential is close to the energy of the resonance state. At this point the current due to electrons is compensated by the current due to holes, so the total current vanishes. In turn, for higher chemical potentials (to the right of the resistance maximum) the particle current dominates and the total current is negative, while for lower chemical potentials (to the left of the resistance maximum) the hole current dominates and current is positive.
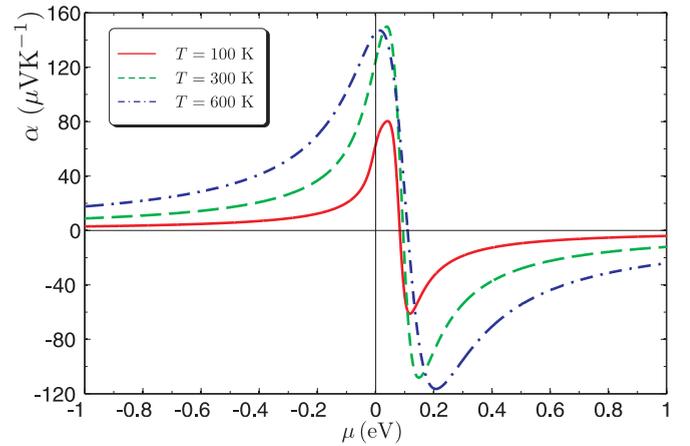

FIG. 3. (Color online) Seebeck coefficient α (thermopower) of graphene as a function of the chemical potential μ for indicated values of temperatures T and for $V_0/V_c = -100$. Other parameters are as described in the main text.

The above described behavior of the thermocurrent and electrical resistivity is also reflected in the dependence of the Seebeck coefficient α on the chemical potential μ. To calculate α, we use Eq. (7) and assume parameters as described above. Chemical potential dependence of α is presented in Fig. 3 for $V_0/V_c = -100$ and for three indicated temperatures. Obviously, the Seebeck coefficient (thermopower) is equal to zero at the chemical potential where the thermocurrent vanishes, i.e., when the chemical potential is close to the resonance levels. For larger chemical potentials, the thermopower is negative since the current is dominated by particles. In turn, for lower chemical potentials the thermopower is positive as the current is then dominated by holes. Interestingly, the maxima in the absolute magnitude of the thermopower appear at the points where the change in the corresponding resistance (and thus also in transmission through the graphene) with the chemical potential reaches a maximum. It should be noted that in the model of nonresonant impurity scattering, Hwang *et al.* [36] also has found a nonlinear temperature dependence and saturation of the thermopower at low carrier density.

Figure 4 shows the corresponding figure of merit ZT, defined as

$$ZT = \frac{T\alpha^2\sigma}{\kappa}, \tag{19}$$

where κ is the total thermal conductivity, which includes both electron and phonon contributions, $\kappa = \kappa_e + \kappa_p$. Figure 4(a) shows the maximum value of ZT, calculated as a function of chemical potential in the limit of $\kappa_p \rightarrow 0$. In turn, Fig. 4(b) presents the figure of merit ZT calculated with the heat conductivity including a nonzero phonon term equal to $\kappa_p = 40 \times 10^{-9}$ W K^{-1}. This conductivity is taken from the experiment [37] performed at the room temperature. It should be mentioned also that the thermal conductivity decreases with decreasing temperature [29]. The thermal conductivity was also measured by Fong *et al.* [38]. The temperature dependence of ZT in Fig. 4(c) is shown for the values of chemical potentials μ corresponding to the maximum value of ZT in Fig. 4(a). Note that the figure of merit is equal to zero for the chemical potential, where the thermopower vanishes (maxima of the
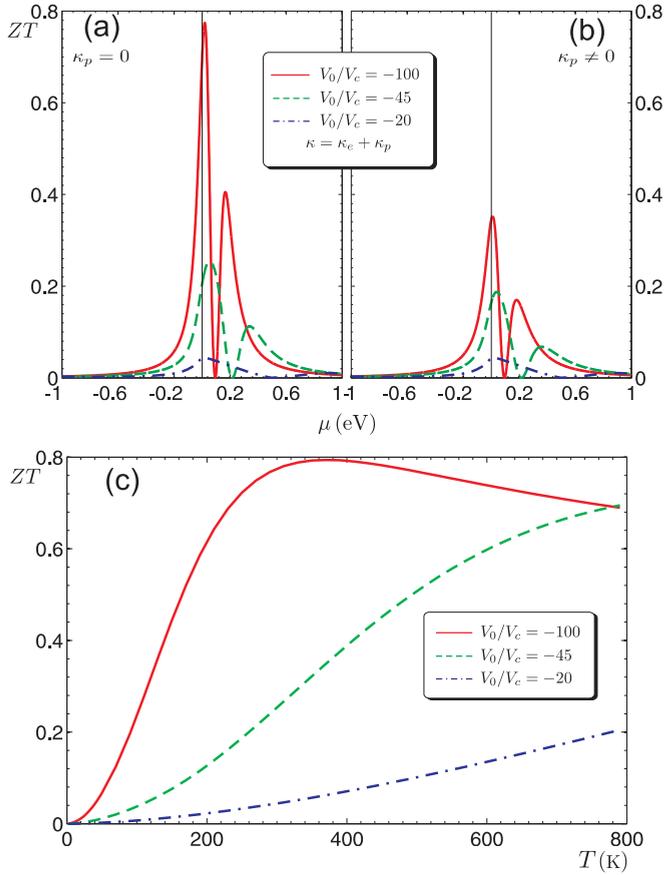
FIG. 4. (Color online) Figure of merit ZT as a function of the chemical potential μ for the neglected phonon term in the thermal conductivity, $\kappa_p = 0$ (a), and with $\kappa_p = 40 \times 10^{-9}$ K^{-1}W (b), calculated for $T = 300$ K and for indicated values of V_0/V_c. (c) Temperature dependence of ZT for $\kappa_p = 0$, and for chemical potentials corresponding to the maxima in ZT from (a). Other parameters are as described in the main text.

resistance). However, there is a significant enhancement of the figure of merit due to the resonant scattering from impurities, and the enhancement appears at the chemical potential where the electrical resistance varies rapidly with μ.

V. THE WIEDEMANN-FRANZ LAW FOR GRAPHENE

Let us consider now the Wiedemann-Franz law. In ordinary metals this law states that the ratio $\kappa/\sigma T$ is constant,

$$\frac{\kappa}{T\sigma} = L, \qquad (20)$$

where $L = L_0 = \pi^2 k_B^2/3e^2 = 2.44 \times 10^{-8}$ W Ω K^{-2} is a constant, known as the Lorentz number. The situation in graphene is different. Strong energy dependence of the relaxation time due to the presence of resonance states leads to a significant dependence of the ratio $\kappa/\sigma T$ on the chemical potential μ, as shown in Fig. 5 for $T = 300$ K and indicated values of the impurity scattering potential V_0. As one can see, this ratio is not constant, but strongly depends on the chemical potential μ, especially in the vicinity of the resonance states. Moreover, the maximum value of this ratio also depends on the impurity potential V_0. However, far from the resonance states, when
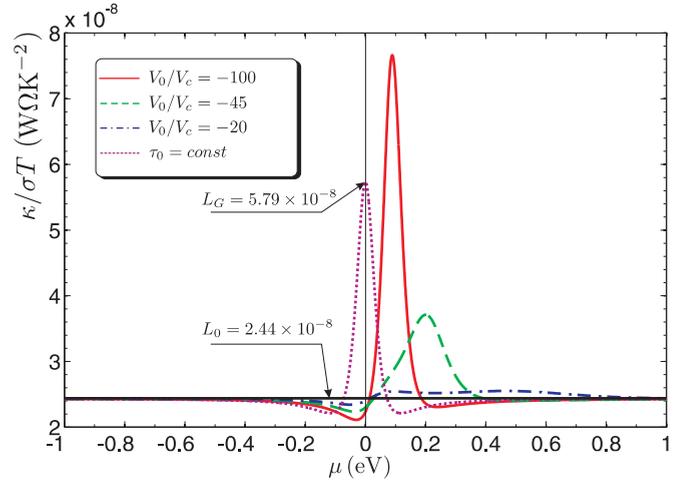

FIG. 5. (Color online) The Wiedemann-Franz ratio as a function of chemical potential μ for $T = 300$ K and for three indicated values of the scattering potential (resonance levels) as well as for a constant relaxation time (dotted line). The black line corresponds to the Lorentz number in metals, $L_0 = 2.44 \times 10^{-8}$ W Ω K^{-2}, whereas $L_G = 5.79 \times 10^{-8}$ W Ω K^{-2} corresponds to the Wiedemann-Franz ratio for graphene at $\mu = 0$ for a constant relaxation time.

the Fermi level is well inside the upper (positive μ) or lower (negative μ) band, the ratio $\kappa/\sigma T$ tends to the number typical for metals, i.e., to L_0. It is rather clear that the deviation of the ratio $\kappa/\sigma T$ from L_0 follows from the resonance states and specific electronic structure of graphene. Similar deviations are also known in other systems, for instance in transport through nanoscopic quantum objects like quantum dots, molecules, and others.

It is interesting to consider the situation which may be directly compared to ordinary metals, i.e., when the relaxation time due to impurity scattering is constant, $\tau = \tau_0$, in the vicinity of the point $\mu = 0$. The corresponding ratio L is shown in Fig. 5. When the chemical level is well inside the valence or conduction bands, $|\mu| \gg 0$, the ratio $\kappa/\sigma T$ tends to the Lorentz number L_0. However, this ratio has a maximum at $\mu = 0$, i.e., at the point where the density of states in graphene disappears. This maximum value at $\mu = 0$ can be calculated analytically assuming that the relaxation time is constant $\tau = \tau_0$ in the vicinity of the point $\mu = 0$. In other words, we assume that one can neglect the dependence of τ on energy, $\delta\tau(\varepsilon)/\tau \ll 1$ for $|\varepsilon| \leqslant k_B T$, which is certainly fulfilled at rather low temperatures for any dependence $\tau(\varepsilon)$. In such a case, the kinetic coefficient $K_{21} = 0$, and the other coefficients can be calculated analytically,

$$K_{11} = \frac{\tau_0 k_B T \ln 2}{2\pi \hbar^2}, \qquad (21)$$

$$K_{31} = \frac{9\zeta(3)\tau_0 k_B^3 T^3}{4\pi \hbar^2}. \qquad (22)$$

Using Eqs. (21) and (22), one can calculate the Lorentz number for graphene at $\mu = 0$,

$$L_G \equiv \frac{\kappa}{\sigma T}\bigg|_{\mu=0} = \frac{9k_B^2 \zeta(3)}{2e^2 \ln 2}, \qquad (23)$$

where $\zeta(x)$ is the Riemann's ζ function. This value of L_G is equal to $5.795\,070\,903 \times 10^{-8}$ W Ω K^{-2}.

Taking into account that $L_0 = \pi^2 k_B^2 / 3e^2$, one finds

$$\frac{L_G}{L_0} = \frac{27\,\zeta(3)}{2\pi^2 \ln 2} \simeq 2.37. \tag{24}$$

This result was obtained earlier by Saito *et al.* [29] for the case of purely ballistic electric and thermal conductance of graphene, when $\mu = 0$. It was also found by Sharapov *et al.* [39].

VI. SUMMARY AND CONCLUSIONS

We have analyzed theoretically the thermoelectric properties of graphene with impurities equally distributed in both A and B sublattices. The assumed impurities lead to resonance impurity states near the Fermi level, and therefore to resonance electron scattering. In agreement with Mott's law, the magnitude of the Seebeck coefficient α and shape of its dependence on the chemical potential are strongly affected be the dependence of the conductivity on μ, which in turn is determined mainly by the electron scattering from impurities in the vicinity of resonance states. These resonant states also lead to a significant enhancement of the figure of merit ZT.

We have also shown that the ratio $\kappa/\sigma T$ deviates from the Lorentz number L_0, and this deviation appears for chemical potentials in the vicinity of the resonant states. Moreover, for a fixed value of the relaxation time we have found an analytical formula for the ratio $\kappa/\sigma T$ at $\mu = 0$, which agrees with that derived earlier.

In our calculations we introduced the impurity density N_i, the impurity scattering potential V_0, and the chemical potential μ as independent parameters. This assumption can be justified if there are other (not necessarily resonant) impurities and defects in graphene. The chemical potential can be also tuned by an external gate voltage, which gives an additional experimental tool to study the thermoelectric properties of graphene and their dependence on the above mentioned parameters.

Our results are in agreement with other works [7,8], and confirm that graphene with resonant impurities can be a perspective material for thermoelectricity. Generally, searching for best thermoelectric materials leads to a requirement of a narrow peak of conductivity as a function of energy, which gives a sharp dependence of the conductivity in a narrow energy region [40,41]. In principle, our results for graphene with resonant impurities leading to a sharp dependence of electron mobility are in agreement with this requirement. However, other scattering mechanisms, such as phonon scattering, can make this dependence weaker, which reduces the thermoelectric parameters. Thus, the predominant resonant impurity scattering could be observed at rather low temperatures, where the phonon scattering is suppressed, and also when other nonresonant scattering processes are reduced. General discussion of different scattering mechanisms in graphene and their relation to transport properties can be found in Ref. [42].

[1] A. H. C. Neto, F. Guinea, N. M. R. Peres, K. S. Novoselov, and A. K. Geim, Rev. Mod. Phys. **81**, 109 (2009).

[2] S. Das Sarma, S. Adam, E. H. Hwang, and E. Rossi, Rev. Mod. Phys. **83**, 407 (2011).

[3] A. A. Balandin, S. Ghosh, W. Bao, I. Calizo, D. Teweldebrahn, F. Miao, and C. Lau, Nano Lett. **8**, 902 (2008).

[4] Y. Xu, Z. Li, and W. Duan, Small **10**, 2182 (2014).

[5] D. Dragoman and M. Dragoman, Appl. Phys. Lett. **91**, 203116 (2007).

[6] T. Stauber and N. M. R. Peres, and F. Guinea, Phys. Rev. B **76**, 205423 (2007).

[7] T. Löfwander and M. Fogelström, Phys. Rev. B **76**, 193401 (2007)

[8] D. Wang and J. Shi, Phys. Rev. B **83**, 113403 (2011).

[9] Y. M. Zuev, W. Chang, and P. Kim, Phys. Rev. Lett. **102**, 096807 (2009).

[10] L. Zhu, R. Ma, Li Sheng, M. Liu, and D.-N. Sheng, arXiv:0908.4302.

[11] X. Z. Yan and C. S. Ting, Phys. Rev. B **81**, 155457 (2010).

[12] S. G. Sharapov and A. A. Varlamov, Phys. Rev. B **86**, 035430 (2012).

[13] L. Hao and T. K. Lee, Phys. Rev. B **82**, 245415 (2010).

[14] M. Wierzbowska, A. Dominiak, and G. Pizzi, 2D Materials **1**, 035002 (2014).

[15] M. Wierzbowska and A. Dominiak, Carbon **80**, 255 (2014).

[16] Z. G. Fthenakis, Z. Zhu, and D. Tomanek, Phys. Rev. B **89**, 125421 (2014).

[17] P. Wei, W. Bao, Y. Pu, C. N. Lau, and J. Shi, Phys. Rev. Lett. **102**, 166808 (2009).

[18] X. Ni, G. Liang, J.-S. Wang, and B. Li, Appl. Phys. Lett. **95**, 192114 (2009).

[19] T. Gunst, T. Markussen, A.-P. Jauho, and M. Brandbyge, Phys. Rev. B **84**, 155449 (2011).

[20] H. Karamitaheri, M. Pourfath, R. Faez, and H. Kosina, J. Appl. Phys. **110**, 054506 (2011).

[21] Y. Yan, Q.-F. Liang, H. Zhao, C.-Q. Wu, and B. Li, Phys. Lett. A **376**, 2425 (2012).

[22] P.-H. Chang and B. Nikolić, Phys. Rev. B **86**, 041406(R) (2012).

[23] M. Wierzbicki, R. Swirkowicz, and J. Barnaś, Phys. Rev. B **88**, 235434 (2013).

[24] L. Liang, E. Cruz-Silva, E. Costa Girão, and V. Meunier, Phys. Rev. B **86**, 115438 (2014).

[25] Z. Aksamija, and I. Knezevic, Phys. Rev. B **90**, 035419 (2014).

[26] W. Chen and A. A. Clerk, Phys. Rev. B **86**, 125443 (2012).

[27] L. Lindsay, Wu Li, J. Carrete, N. Mingo, D. A. Broido, and T. L. Reinecke, Phys. Rev. B **89**, 155426 (2014).

[28] B. D. Kong, S. Paul, M. B. Nardelli, and K. W. Kim, Phys. Rev. B **80**, 033406 (2009).

[29] K. Saito, J. Nakamura, and A. Natori, Phys. Rev. B **76**, 115409 (2007).

[30] S. Yiğen, V. Tayari, J. O. Island, J. M. Porter, and A. R. Champagne, Phys. Rev. B **87**, 241411(R) (2013).

[31] A. Principi and G. Vignale, arXiv:1406.2940.

[32] C. L. Kane and E. J. Mele, Phys. Rev. Lett. **95**, 226801 (2005).

[33] P. S. Kireev, *Semiconductor Physics* (Mir Publishers, Moscow, 1974).

[34] G. D. Mahan, *Many Particle Physics* (Plenum, New York, 2009).

[35] M. Inglot and V. K. Dugaev, J. Appl. Phys. **109**, 123709 (2011).

[36] E. H. Hwang, E. Rossi, and S. Das Sarma, Phys. Rev. B **80**, 235415 (2009).

[37] J. H. Seol, I. Jo, A. L. Moore *et al.*, Science **328**, 213 (2010).

[38] K. C. Fong, E. E. Wollman, H. Ravi, W. Chen, A. A. Clerk, M. D. Shaw, H. G. Leduc, and K. C. Schwab, Phys. Rev. X **3**, 041008 (2013).

[39] S. G. Sharapov, V. P. Gusynin, and H. Beck, Phys. Rev. B **67**, 144509 (2003).

[40] G. D. Mahan and J. O. Sofo, Proc. Natl. Acad. Sci. USA **93**, 7436 (1996).

[41] J. Zhou, R. Yang, G. Hen, and M. S. Dresselhaus, Phys. Rev. Lett. **107**, 226601 (2011).

[42] M. I. Katsnelson, *Graphene: Carbon in Two Dimensions* (Cambridge Univsity Press, Cambridge, 2012), Chap. 11.